

Simultaneous multimodality molecular imaging with neodymium-doped $\text{Y}_3\text{Al}_5\text{O}_{12}$ nanoparticles

YONGHUA ZHAN^{a,#}, XU CAO^{a,#}, XIN CAO^a, FEI KANG^c, JING WANG^c, JIMIN LIN^a, ZHIMIN LI^{b,*}, XUELI CHEN^{a,*}

^aEngineering Research Center of Molecular and Neuro Imaging of the Ministry of Education & School of Life Science and Technology, Xidian University, Xi'an, Shaanxi 710071, China

^bSchool of Advanced Materials and Nanotechnology, Xidian University, Xi'an, Shaanxi 710071, China

^cDepartment of Nuclear Medicine, Xijing Hospital, Fourth Military Medical University, Xi'an, Shaanxi 710032, China

[#]These authors contributed equally to this work

Capturing simultaneously multimodality information using one imaging agent is a new direction of molecular imaging technology. In this work, we report a proof-of-concept study that uses trimodality imaging consisting of fluorescence imaging (FI), X-ray excited luminescence imaging (XEL), and radionuclide excited luminescence imaging (REL), with the injection of only one kind of $\text{Nd}^{3+}:\text{Y}_3\text{Al}_5\text{O}_{12}$ nanoparticles. The spectrum measurements and the results of *in vivo* pseudo-tumor based experiments validated the capability of $\text{Nd}^{3+}:\text{Y}_3\text{Al}_5\text{O}_{12}$ nanoparticles as agents for trimodality imaging. This proof-of-concept study may open the door for the rapid development of multimodality imaging technology that facilitates the acquisition of a large novel information to be simultaneously obtained using one imaging agent and one imaging system.

(Received October 22, 2015; accepted September 29, 2016)

Keywords: Multimodality imaging, Simultaneous imaging, $\text{Nd}^{3+}:\text{Y}_3\text{Al}_5\text{O}_{12}$ nanoparticles

1. Introduction

Neodymium-doped yttrium aluminium garnet ($\text{Nd}^{3+}:\text{Y}_3\text{Al}_5\text{O}_{12}$), a vital laser material, has been widely used for its good optical properties ever since garnet crystals, doped with trivalent rare Nd^{3+} ions, were first discovered by Guesic in 1964 [1]. In recent years, $\text{Nd}^{3+}:\text{Y}_3\text{Al}_5\text{O}_{12}$ lasers have been applied with remarkable success in various industrial fields such as metal processing, single crystal synthesis, and medical operations, especially in clinical practice [2]. It is worth nothing that $\text{Nd}^{3+}:\text{Y}_3\text{Al}_5\text{O}_{12}$ laser has gained a great importance in the field of medicine for the excision, vaporization, and irradiation of tumors [3]. In addition, it also has an impressive ability of stanching the alimentary canal and destroy of the gallstones, which proves that the $\text{Nd}^{3+}:\text{Y}_3\text{Al}_5\text{O}_{12}$ laser has many advantages and will be a very useful tool for surgeons, too [4]. Although it has been used widely in the medical field, little is known whether or not $\text{Nd}^{3+}:\text{Y}_3\text{Al}_5\text{O}_{12}$ particles can be used for medical imaging.

In this study, we report a proof-of-concept study of simultaneously utilizing three types of imaging, including fluorescence imaging (FI), X-ray-excited luminescence imaging (XEL), and radionuclide-excited luminescence imaging (REL), with a single injection of $\text{Nd}^{3+}:\text{Y}_3\text{Al}_5\text{O}_{12}$ nanoparticles. First, the $\text{Nd}^{3+}:\text{Y}_3\text{Al}_5\text{O}_{12}$

nanoparticles were synthesized, and then characterized with a scanning electron microscope (SEM) and an X-ray diffractometer (XRD). Subsequently, the utility of $\text{Nd}^{3+}:\text{Y}_3\text{Al}_5\text{O}_{12}$ nanoparticles in the trimodality imaging (FI, XEL, and REL) was demonstrated by spectrum measurements of the three types of imaging. Finally, the feasibility and potential of the $\text{Nd}^{3+}:\text{Y}_3\text{Al}_5\text{O}_{12}$ nanoparticles-based trimodality imaging were evaluated *in vivo* with a group of pseudo-tumor-based experiments. Our findings offer an alternative route for simultaneously providing molecular and functional information by FI, XEL, and REL signals using an optical imaging device.

2. Experimental

2.1. Synthesis of $\text{Nd}^{3+}:\text{Y}_3\text{Al}_5\text{O}_{12}$

The $\text{Nd}^{3+}:\text{Y}_3\text{Al}_5\text{O}_{12}$ nanoparticles were prepared by a co-precipitation method [5, 6]. Ammonium aluminum sulfate ($\text{NH}_4\text{Al}(\text{SO}_4)_2 \cdot 12\text{H}_2\text{O}$, 99.99 %) and yttrium nitrate ($\text{Y}(\text{NO}_3)_3 \cdot 6\text{H}_2\text{O}$, 99.99 %) were dissolved in distilled water. Neodymium oxide (Nd_2O_3 , 99.99 %) was dissolved in dilute nitric acid. The above solutions were mixed in a molar ratio of $\text{Y}^{3+}:\text{Al}^{3+}:\text{Nd}^{3+} = 2.99:5:0.01$. Ammonium hydrogen carbonate (NH_4HCO_3) was used as a precipitant and dissolved in distilled water. The $\text{Y}^{3+}:\text{Al}^{3+}:\text{Nd}^{3+}$ starting

solution was then dropped into the NH_4HCO_3 solution at a speed of about 2 drops per sec and stirred at 70 °C. The precipitate obtained after filtration was washed with distilled water and alcohol. After drying the precipitate at 80 °C for 24 hours in a vacuum dryer, a loose precursor was obtained and then calcined at 1000 °C for 2 hours.

2.2. Characterization of $\text{Nd}^{3+}:\text{Y}_3\text{Al}_5\text{O}_{12}$

The characterization of $\text{Nd}^{3+}:\text{Y}_3\text{Al}_5\text{O}_{12}$ was measured with an X-ray diffractometer (DX-1000, Dandong Fangyuan Instrument Co. Ltd., Dandong, China) that was used to obtain the crystalline phase of the as-prepared powder. The size and morphology of the $\text{Nd}^{3+}:\text{Y}_3\text{Al}_5\text{O}_{12}$

particles were observed with a scanning electronic microscope (SEM; JSM-6360LV, JEOL, Tokyo, Japan).

3. Results and discussion

The size and morphology of the $\text{Nd}^{3+}:\text{Y}_3\text{Al}_5\text{O}_{12}$ particles were observed with SEM and one of the representative images is shown in Fig. 1 (a). It can be seen that the average size of the particles is about 100 nm, presenting a spherical appearance with slight agglomeration. Meanwhile, the prepared particles were well crystallized. The XRD patterns, describing the crystallite phase of $\text{Nd}^{3+}:\text{Y}_3\text{Al}_5\text{O}_{12}$, are presented in Fig. 1 (b). As can be seen, in the generated powder, there is only the $\text{Nd}^{3+}:\text{Y}_3\text{Al}_5\text{O}_{12}$ phase without other impurities.

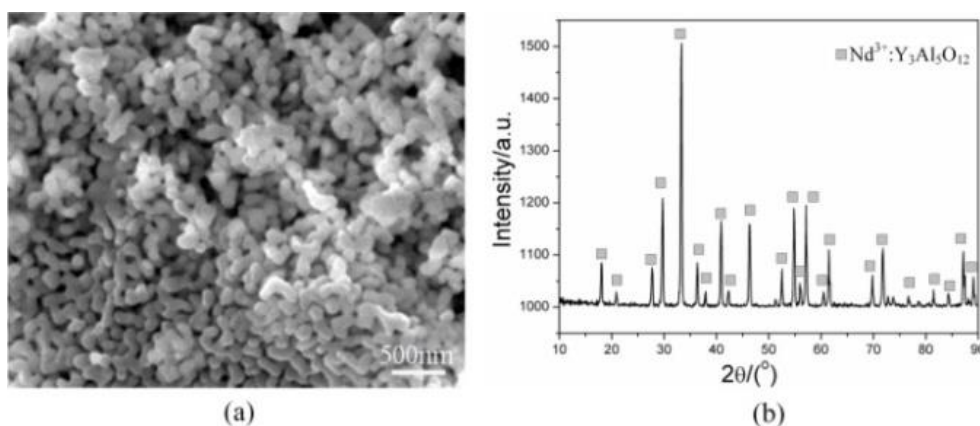


Fig. 1. Characterization of $\text{Nd}^{3+}:\text{Y}_3\text{Al}_5\text{O}_{12}$. (a) SEM image; (b) XRD patterns

To reveal the ability of the $\text{Nd}^{3+}:\text{Y}_3\text{Al}_5\text{O}_{12}$ nanoparticles to serve as a trimodality imaging agent, the spectra of the three types of imaging were recorded when excited by near-infrared light, X-rays, and γ -rays, respectively. The absorption spectrum of $\text{Nd}^{3+}:\text{Y}_3\text{Al}_5\text{O}_{12}$ was measured at 850 nm with a UV-VIS-NIR absorption spectrophotometer (UV-2450, Shimadzu Corporation, Kyoto, Japan). Based on the measured absorption spectrum, the fluorescence spectrum of $\text{Nd}^{3+}:\text{Y}_3\text{Al}_5\text{O}_{12}$ was recorded with a fiber spectrometer (Maya 2000, Ocean Optics, Inc., FL, USA), as shown in Fig. 2 (a). The XEL spectrum was detected with a homemade dual-modality imaging system of optical and X-ray computed tomography [7], using an X-ray source (Apogee, Oxford Instruments, Oxfordshire, UK) to excite $\text{Nd}^{3+}:\text{Y}_3\text{Al}_5\text{O}_{12}$, and an EMCCD camera (iXon Ultra 888, Andor Technology Ltd., Belfast, UK) coupled with a focus lens (Xenon 25 mm f/0.95, Schneider Optics, Inc., CA, USA) to acquire the XEL signals. An epoxy epoxide (EP) tube containing 1 mg $\text{Nd}^{3+}:\text{Y}_3\text{Al}_5\text{O}_{12}$ was placed within the scope of the X-ray beam generated from the X-ray source with a voltage of 50 kV and a current of 1 mA, and XEL at different spectra were captured using a set of narrow band-

pass filters (spectra range of 500-850 nm with an interval of 20 nm and a bandwidth of 10 ± 2 nm, Rayan, China) with an EM gain of 1,000 and an exposure time of 10 s. The resultant spectrum is shown in Fig. 2 (b).

To measure the REL spectrum of $\text{Nd}^{3+}:\text{Y}_3\text{Al}_5\text{O}_{12}$ excited by γ -rays, an EP tube containing 7.4 MBq (200 μCi) ^{18}F -FDG, with a volume of 200 μL , was used as an excitation source. When the other EP tube containing 1 mg of $\text{Nd}^{3+}:\text{Y}_3\text{Al}_5\text{O}_{12}$ was placed near the former one, the radionuclide-excited luminescence signal at different spectra was captured using the same system measuring the XEL spectrum, which is demonstrated in Fig. 2 (c). Fluorescence spectrum, under the excitation light of 850 nm, exhibits two apparent peaks around the wavelengths of 945 nm and 1,064 nm. Although the emission light around these peaks are out of the so-called ideal "optical window" [8, 9], they can play a role in some applications. Fluorescence spectra can be used for biomedical imaging because of the acceptable absorption of water and the low absorption of oxyhemoglobin and hemoglobin, which facilitates a better penetration depth into tissues. On the other hand, Fluorescence spectra may also be used for photothermal therapy, especially at wavelengths beyond

1,000 nm [10-12]. In addition, the produced thermal signals may generate an acoustic wave that can be used for photoacoustic imaging [13-15]. Luminescence spectra emitted under the bombardment of X-rays and γ -rays differ from each other, with the peak wavelength located at 600 nm for X-ray-excited luminescence imaging and 560 nm for REL (as shown in Fig. 2 (b) and (c)), which exhibits different characteristics as compared with other rare-earth nanoparticles, such as $\text{Gd}_2\text{O}_2\text{S:Tb}$ [16-17]. This feature may provide a perfect alternative to simultaneous imaging of positron emission tomography (PET) and

computed tomography (CT), because the XEL and REL may be regarded as providing equivalent information of CT and PET images, respectively. In the traditional dual-modality PET-CT imaging, simultaneous imaging can hardly be achieved because the PET detector is most likely damaged by X-ray bombardment. Thus, using the multi-channel signal detection instrument in which narrow band-pass filters with different central wavelengths are equipped, the XEL and REL can be acquired simultaneously and separately.

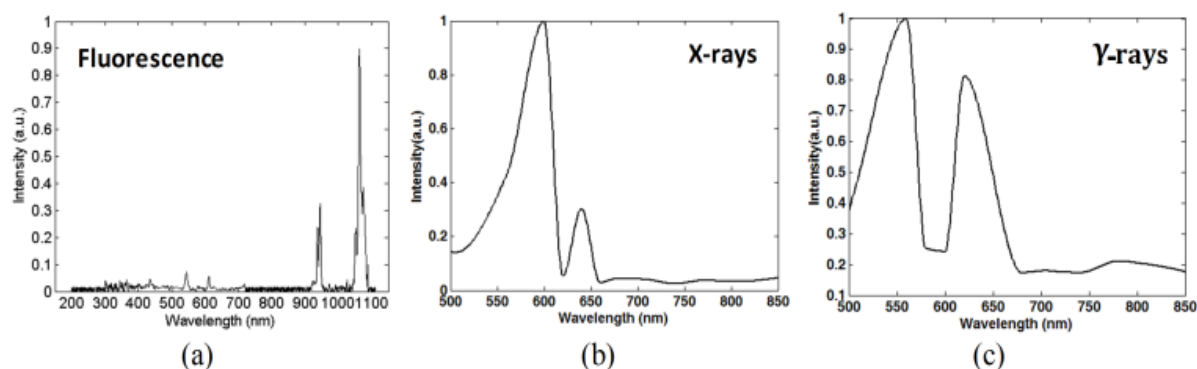


Fig. 2. Emission spectrum of the $\text{Nd}^{3+}:\text{Y}_3\text{Al}_5\text{O}_{12}$. (a) Fluorescence spectrum excited by 850 nm light; (b) X-ray-excited luminescence spectrum; (c) Radionuclide-excited luminescence spectrum

To verify the *in vivo* imaging capacity of $\text{Nd}^{3+}:\text{Y}_3\text{Al}_5\text{O}_{12}$ nanoparticles as trimodality imaging agents, a subcutaneous pseudo tumor model-based animal experiment was conducted, which was accomplished according to previous studies [18]. The pseudo tumor was formed in the back of mouse by subcutaneously injecting the mixture of 1 mg $\text{Nd}^{3+}:\text{Y}_3\text{Al}_5\text{O}_{12}$ and 20 μL of liquid agarose. First, we used a near infrared light beam of 850 nm wavelength to illuminate the mouse. A band-pass filter with a central wavelength of 1,064 nm and a bandwidth of 10 ± 2 nm was used to smooth the emitted fluorescent signals and the fluorescence image was acquired. The CCD camera worked with the electron multiplying (EM) gain of 1 and exposure time of 2 s. Secondly, the X-ray was used as the excitation source, and the CCD camera coupled with a focus lens was used to capture the XEL signals with an EM gain of 1,000 and exposure time of 1 s. Considering that the X-rays have little influence on the XEL image, no filter was adopted in this imaging experiment. Finally, the REL image was also captured half an hour following the injection of 100 μL of 3.7 MBq (100 μCi) ^{18}F -FDG into the tail vein. For the same reason, there was no filter used when the CCD camera collected the REL signals. The EM gain and exposure time were set as 1,000 and 60 s, respectively for the CCD camera. The acquired images for FI, XEL, and REL imaging are shown in Fig. 3 (a), 3 (b), and 3 (c), respectively.

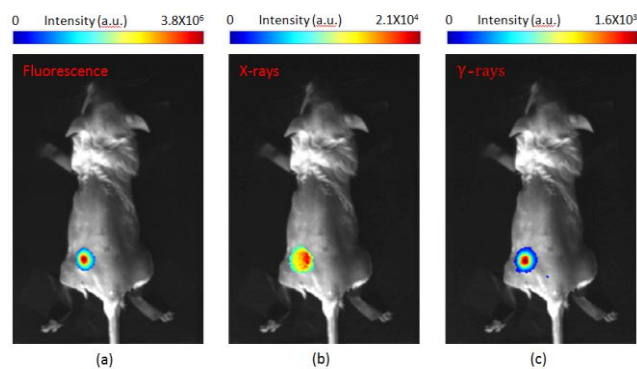


Fig. 3. Imaging results of the subcutaneous pseudo tumor model-based living animal experiment. (a) Image of fluorescence imaging (FI), (b) Image of X-ray-excited luminescence imaging, (c) Image of radionuclide-excited luminescence imaging.

The results of the pseudo tumor-based animal experiment demonstrate the potential application of $\text{Nd}^{3+}:\text{Y}_3\text{Al}_5\text{O}_{12}$ nanoparticles as imaging agents in trimodality imaging *in vivo*. In the acquired images, the fluorescence image exhibits the highest intensity of signals, while the XEL image displays the second highest intensity, and the REL image has the lowest intensity. This reveals that the greatest luminescence yield of $\text{Nd}^{3+}:\text{Y}_3\text{Al}_5\text{O}_{12}$ nanoparticles is obtained with the excitation of infrared light, and the worst yield is for REL imaging. Fortunately, the signals can be captured

by an optical imaging instrument, even for low-intensity signals of REL. The lowest intensity of the REL may be due to the insufficient excitation source of γ -rays. For a pseudo tumor that was used for imaging in this proof-of-concept study, the ^{18}F -FDG could not converge spontaneously around the pseudo tumor. As a result, the nanoparticles inside the pseudo tumor can only be further excited by the γ -rays emitted from some distant radionuclides. The further the distance of the nanoparticles from the radionuclides, the lower the intensity of radionuclide-excited luminescence is obtained. If the nanoparticles and radionuclides are bound in one probe, the intensity of emitted radionuclide-excited luminescence would be greatly improved. Thus, we observed that the pseudo tumor-based animal experiment validated the availability of $\text{Nd}^{3+}:\text{Y}_3\text{Al}_5\text{O}_{12}$ nanoparticles as agents for *in vivo* trimodality imaging.

4. Conclusions

To summarize, a proof-of-concept study utilizing three types of imaging to be performed with a single agent, has been reported using the neodymium-doped yttrium aluminium garnet ($\text{Nd}^{3+}:\text{Y}_3\text{Al}_5\text{O}_{12}$). The trimodality imaging includes fluorescence imaging (FI), X-ray-excited luminescence imaging (XEL), and radionuclide-excited luminescence imaging (REL). The spectrum measurements and a pseudo-tumor-based *in vivo* experiment demonstrated the feasibility of this proof-of-concept study. Since XEL and REL compliment the processes of CT and PET, they can be regarded as an equivalent form of technology to obtain similar information. As a result, this study promotes three types of imaging that provide five kinds of information (fluorescence, XEL, REL, equivalent PET, and equivalent CT information) with a single injection of an imaging agent. The $\text{Nd}^{3+}:\text{Y}_3\text{Al}_5\text{O}_{12}$ nanoparticles may open the door for multimodality imaging technology and promote the development of a multimodality imaging system that allows new information to be obtained using simultaneously one imaging agent and one imaging system, [19]. Our future work will focus on the functional specificity of nanoparticles by synthesizing the targeted probes and the extension of these nanoparticles for *in vivo* applications.

Acknowledgments

This work was partly supported by the National Natural Science Foundation of China under Grant Nos. 81101100, 81227901, 81571725, 81230033, 81090272, 81101083, 31371006, 61405149, 81401442, the Natural Science Basic Research Plan in Shaanxi Province of China under Grant No. 2015JZ019, 2015JQ6249,

Ningbo Natural Science Foundation under Grant No. 2015A610037, and the Fundamental Research Funds for the Central Universities (NSIZ021402, NSIY061406).

References

- [1] E. A. Seregina, A. A. Seregin, *Quantum. Electron* **43**, 150 (2013).
- [2] D. Y. Kosyanov, V. N. Baumer, R. P. Yavetskiy, V. L. Voznyy, V. B. Kravchenko, Y. L. Kopylov, A. V. Tolmachev, *Crystallogr. Rep.* **60**, 299 (2015).
- [3] J. G. Li, T. Ikegami, J. H. Lee, T. Mori, Y. Yajima, J. *Eur. Ceram. Soc.* **20**, 2395 (2000).
- [4] A. Ikesue, *Opt. Mater* **19**, 183 (2002).
- [5] S. H. Tong, T. C. Lu, W. Guo, *Mater. Lett.* **61**, 4287 (2007).
- [6] G. G. Xu, X. D. Zhang, W. He, H. Liu, H. Li, R. I. Boughton, *Mater. Lett.* **60**, 962 (2006).
- [7] X. Chen, X. Gao, D. Chen, X. Ma, X. Zhao, M. Shen, X. Li, X. Qu, J. Liang, J. Ripoll, J. Tian, *Opt. Express* **18**, 19876 (2010).
- [8] T. Niidome, M. Yamagata, Y. Okamoto, Y. Akiyama, H. Takahashi, T. Kawano, Y. Katayama, Y. Niidome, *J. Control. Release* **114**, 343 (2006).
- [9] T. G. Phan, A. Bullen, *Immunol. Cell. Biol.* **88**, 438 (2010).
- [10] J. L. Boulnois, *Lasers. Med. Sci.* **1**, 47 (1986).
- [11] M. H. Khan, R. K. Sink, D. Manstein, D. Eimerl, R. R. Anderson, *Laser. Surg. Med.* **36**, 270 (2005).
- [12] G. Shan, R. Weissleder, S. A. Hilderbrand, *Theranostics* **3**, 267 (2013).
- [13] K. Wilson, K. Homan, S. Emelianov, *Nat. Commun.* **3**, 618 (2012).
- [14] L. V. Wang, S. Hu, *Science* **335**, 1458 (2012).
- [15] J. R. Rajian, R. Li, P. Wang, J. X. Cheng, *J. Phys. Chem. Lett.* **4**, 3211 (2013).
- [16] H. Chen, T. Moore, B. Qi, D. C. Colvin, E. K. Jelen, D. A. Hitchcock, J. He, O. T. Mefford, J. C. Gore, F. Alexis, J. N. Anker, *Acs. Nano.* **7**, 1178 (2013).
- [17] X. Cao, X. Chen, F. Kang, Y. Zhan, X. Cao, J. Wang, J. Liang, J. Tian, *Acs. Appl. Mater. Inter.* **7**, 11775 (2015).
- [18] H. G. Liu, X. F. Zhang, B. G. Xing, P. Z. Han, S. S. Gambhir, Z. Cheng, *Small.* **6**, 1087 (2010).
- [19] C. Li, Y. Yang, G. S. Mitchell, S. R. Cherry, *J. Nucl. Med.* **52**, 1268 (2011).

*Corresponding author: xlchen@xidian.edu.cn,
lizhmin@163.com